COMAT

The 9th International Conference on Advanced Composite Materials Engineering

Transilvania University of Brasov
FACULTY OF MECHANICAL ENGINEERING

17-18October 2022

CFD MODEL FOR FREE-FLOW SIMULATION OF WIND TURBINE BLADES

Tollár S.[1]

1.Institute of Energy Engineering and Chemical Machinery, University of Miskolc, Miskolc, Hungary, sandor.tollar@uni-miskolc.hu

Abstract: *The aim of this article is to define the setup parameters for the ANSYS Fluent CFD simulation, which is able to calculate the lift and drag forces acting on an airfoil in free flow with high accuracy. In further research, we intend to apply the model to the simulation of turbine blade icing, with the aim of identifying profiles that are less sensitive to icing. The airfoil under investigation is the NACA series 4412 airfoil and the tests were performed with Re = 10^6. Our investigations include the definition of the computational domain, the mesh settings, the choice of the turbulence model and the formulation of the convergence criteria. Our results were compared with published computational and measurement data. The conclusions drawn from the comparison are summarized.*

Keywords: *turbulence models, lift force, drag force*

1. INTRODUCTION

Wind turbines operate under extreme operating conditions. One of the environmental effects is a phenomenon that can change the basic operating parameters of turbines. This is icing. If ice forms on the surface of the blades, the blade contours are no longer the ones designed for the flow. The flow around the changed icy contour will produce less lift, but the drag will be higher. Practical experience has shown that severe icing can result in a complete turbine shutdown and that ice can remain on the blades much longer than the formation of icing conditions. Therefore, annual power losses can increase to as much as 20-50 % in harsh locations [1-5].

Several alternatives for protecting shovels against icing have been developed over the past decades. We now want to approach the problem from a different direction. The subject of our research is to investigate the sensitivity of blade profiles to icing. As a first step, we investigated the simulation of a non-icing profile, which will be suitable for the simulation of iced profiles in the future.

2. MAIN PARAMETERS OF THE SIMULATION TEST MODEL FOR AIRFOILSS

The first phase of the research is to build a simulation that calculates the buoyancy and drag coefficients that are important to us, according to known measurements and research results.
For the tests we used the academic version of the ANSYS Fluent 19R3 software, which is available at our institute. The study was carried out in the form of a 2-D model test. The Reynolds number was $Re = 10^6$ and the reference deflection angle was 10°.
Once the geometry is fixed, the test range is determined. A hybrid mesh is developed that best suits the nature of the task: a structured mesh is used near the profile, and an unstructured mesh is used for the rest of the domain. The boundary conditions are then defined, and the turbulence model is selected, based on recommendations from the literature, and simulations are performed, the results of which are compared with published computational and measurement data. At the end of the process, all simulation parameters will be recorded for future studies.

a. The geometry under consideration

The profile we use is the NACA4412 profile with L = 1 m chord length. We chose this profile because there is ample reference data available for this profile, and it was also the subject of the icing study by Kollar and Mishra [6], which we used as a starting point.

b. Meshing

To solve the problem, we first had to define the 2-D domain - domain - where we wanted to perform the calculations. Based on the recommendations in the literature, a "D" shaped domain was formed around the profile to be investigated, the geometric dimensions of which were determined in relation to the chord length [7, 8]. The radius of the circular leading edge of the domain is $12.5 \cdot L$, the length of the domain after the semicircular domain is also $12.5 \cdot L$. The profile is positioned at the origin of the circular arc. The circular arc boundary of the domain with the tangentially parallel boundary lines forms the inlet surface, the inlet. The rear vertical terminating line of the range forms the exit surface, the outlet.
In the cases under consideration, the Reynolds number is 10^6, so we should expect turbulence. The turbulence is generated in the boundary layer, in our case along the surface of the profile in free flow. To study the boundary layer, a mesh constructed of multilayer prismatic elements is required. The number of layers and their thickness depends on the thickness of the

boundary layer, its structure, and the method used to model the boundary layer conditions.

i. Treatment of the boundary layer in the simulation

The treatment of the boundary layer is a crucial issue for our simulation, so more attention will be devoted to its description. Basically, the boundary layer can be divided into two parts, the inner boundary layer, and the outer boundary layer [9, 10]. The inner boundary layer can be further divided into the viscous sublayer directly connected to the wall, and the turbulent log-layer and the buffer layer located in front of the outer boundary layer. In practice, two basic solutions to deal with the boundary layer have been widely used: the use of wall functions and the viscous layer solution.

2.1 Use of wall functions

The boundary layer profile is used in this method. To determine the values for the cells adjacent to the wall, such as the shear stress, the center of the cell must fall within the log-layer. For this to be true, the first node must be taken between $y+ = 30$ and 300 (the cell center will then be between $y+ = 15$ and 150, which falls in the log-layer. This method can be used with good results if the aim is to calculate the mixing in the middle of the domain rather than to determine the forces on the wall.

2.2 Solution of the viscous layer

For the mesh to be able to handle gradients properly, the first grid size must be $y+ = 1$ and the grid growth factor must not be greater than 1.2. This method requires a much larger number of cells, so the computation time increases significantly. The aim of our research is to investigate iced-up profiles, so we decided that although for smooth profiles the use of wall features gives good results with significantly lower computational requirements, we will use the viscous layer solution from the beginning for future comparability. The profile proximity prismatic mesh constructed using this method is shown in Figure 1 left side.

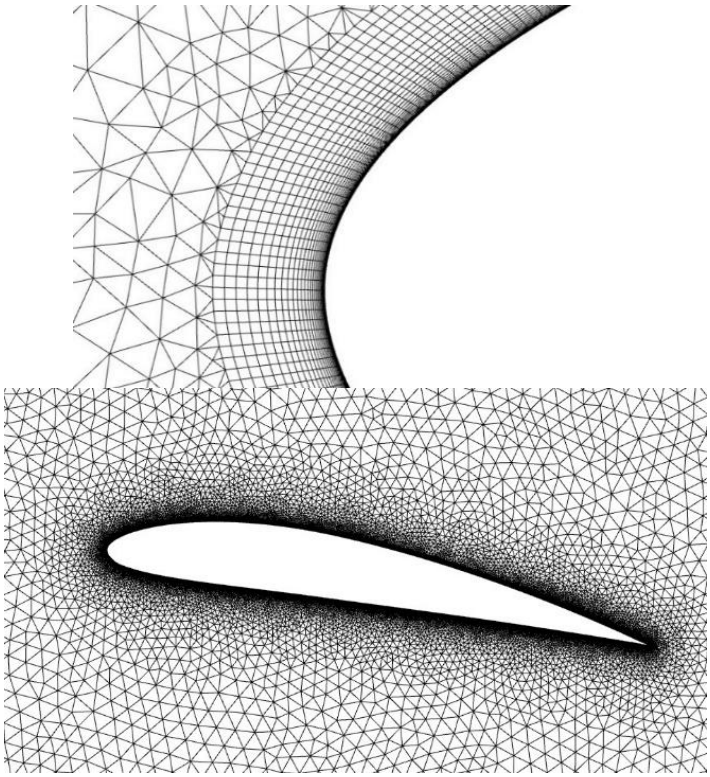

1. Figure: The hybrid mesh around the profile

c. Boundary conditions and simulation settings

On the contour of the airfoil, a Dirichlet boundary condition is imposed on the velocity values and a Neumann boundary condition is imposed on the pressure. The inlet surface of the flow was defined as velocity input and the outlet surface as pressure output. The flowing medium is air. A pressure-based solution scheme was used since the Mach number of the flow is below 0.3. The damping factor of all transport variables is set to 0.8. The initialization of the solution was calculated from the inlet surface. A convergence criterion of 10^{-5} was imposed to solve the equations, which must be satisfied for all residual values. To model the flow around a free-flowing profile, different turbulence models are proposed in the literature even at high Reynolds number. Each model has certain advantages over the others in terms of computational capacity, run time, accuracy of results. In the 2D simulations, we used the turbulence models of RANS (Reynolds-Averaged Navier-Stokes Simulation).

d. Introduction to RANS (Reynolds-Averaged Navier-Stokes Simulation)

RANS is the most widely used approach for modelling industrial flows and is suitable for representing turbulent motion. The time-averaged flow and turbulence levels provide sufficient information to calculate the buoyancy and drag coefficients of interest. The computational complexity is lower compared to LES for a well-structured mesh and appropriate parameters. Based on all these considerations, we further searched for a suitable turbulence model within the possibilities offered by RANS. The time-averaged equations used in RANS are as follows [11]

Mass conservation (continuity):

$$\frac{\partial \rho}{\partial t} + \frac{\partial}{\partial x_i}(\rho u_i) = 0, \tag{1}$$

Conservation of momentum (Navier-Stokes equations):

$$\frac{\partial}{\partial t}(\rho u_i) + \frac{\partial}{\partial x_i}(\rho u_i u_j) = -\frac{\partial p}{\partial x_i} + \frac{\partial}{\partial x_j}\left[\mu\left(\frac{\partial u_i}{\partial x_i} + \frac{\partial u_j}{\partial x_i} - \frac{2}{3}\delta_{ij}\frac{\partial u_l}{\partial x_l}\right)\right] + \frac{\partial}{\partial x_j}\left(-\rho\overline{u_i' u_j'}\right). \tag{2}$$

However, the Reynolds averaged approach to turbulence requires that the Reynolds stresses in equation (2) are properly modelled. Due to the higher order non-linear terms, the equations are not closed. A commonly used method for relating Reynolds stresses to average velocity gradients is the Boussinesq hypothesis [11]:

$$-\rho\overline{u_i' u_j'} = \mu_t\left(\frac{\partial u_i}{\partial x_j} + \frac{\partial u_j}{\partial x_i}\right) - \frac{2}{3}\left(\rho k + \mu_t \frac{\partial u_k}{\partial x_k}\right)\delta_{ij}. \tag{3}$$

Within the RANS method there are several different models available in ANSYS Fluent, the most commonly used ones for the given task are Spalart-Allmaras, Realizable *k-ε*, Standard *k-ω*, SST *k-ω* methods. Most of them use the Boussinesq hypothesis to close the Navier-Stokes equations. The advantage of this approach is that the turbulent viscosity, μ_t, is relatively low computationally demanding to calculate. For the Spalart-Allmaras model, only one additional transport equation (representing the turbulent viscosity) is solved, whereas for the *k-ε* and *k-ω* models, 2-2 transport equations are required. [11, 12]

The review shows that all four methods are suitable for calculations around the profile under certain conditions. Not all possible options within RANS have been explored. The aim is to select an efficient but good approximation method for further simulation studies. An important consideration was to keep the computational requirements as low as possible. Since some literature performs simulations of the flow around an airfoil in the flow assuming a steady flow in time, we have performed calculations in two cases with this setting. In this way, six different models were used to determine the pressure distribution and coefficients around the airfoil. The models tested are shown in Table 1. To assess the applicability of these turbulence models, a comparative study was carried out to select the turbulence model to be used in further simulations.

3. COMPARISON OF THE SIMULATIONS

The simulation tests were carried out as 2-D simulations, with Reynolds number $Re = 10^6$ and angle of deflection $\alpha = 10°$. Simulation results of the NACA4412 airfoil using the XFOIL program of the public Airfoil Tools portal were used as a reference [13, 14]. The data include the lift coefficient and drag coefficient for $Re = 10^6$. Our results were also compared with measured data. As a reference, the measurement results of Abbott and von Doenhoff were used [15]. For the transient simulations we set a time step of $5 \cdot 10^{-3}$ s with 20,000 steps. The steady simulations were run up to 5,000 iterations. For the transient simulations, the residuals were set to 10^{-5}. The simulation tests were performed sequentially, and the results are summarized with the reference data in Table 1.

1. Table: Comparison of the results obtained with the tested turbulence models

turbulence models	***Cd***	***Cl***
Spalart- Allmaras (steady)	0.0364	1.212
k-ω Standard (steady)	0.0396	1.171
k-ε realizable (transient)	0.0343	1.160
Spalart – Allmaras (transient)	**0.0327**	**1.230**
k-ω Standard (transient)	**0.0305**	**1.369**
k-ω SST (transient)	**0.0368**	**1.179**
Abbott (exp. ref.) [15]	*0.0175*	*1.378*
XFOIL (ref.) [14]	*0.0175*	*1.432*

4. CONCLUSIONS

Based on our experience, all settings converged to *Cl* and *Cd* values. All methods led to valuable results. For our further investigations, we choose among the Spalart-Allmaras, the *k-ω* standard and the *k-ω* SST methods for transient models. The lift force calculated with these models are the closest to the reference values. However, further investigations are needed because the calculated drag forces deviated significantly from the references.

Further tests will be performed at $Re = 3 \cdot 10^6$ and compared with additional measured data to select a turbulence model for future icing studies.

REFERENCES

[1] L. Battisti, R. Fedrizzi, A. Brighenti, T.Laakso: Sea ice and icing risk for offshore wind turbines, Owemes 2006, 20-22 April. Citavecchia, Italy

[2] Laakso, T., Holttinen, H., Ronsten, G., Horbaty, R., Lacroix, A., Peltola, E., Tammelin, B.: State-of-the-art of wind energy in cold climates, http://arcticwind.vtt.fi, 2003.

[3] Tammelin, B., Cavaliere, M., Holtinnen, H., Morgan, C., Seifert, H.: Wind Energy in Cold Climate, Final Report WECO (JOR3-CT95-0014) ISBN 951-679-518-6, Finnish Meteorological Institute, Helsinki, Finland, 2000.

[4] Bose, N., Rong, J. Q.: Power reduction from ice accretion on a horizontal axis wind turbine, Proc.12th British Wind Energy Association, Wind Energy Conference Norwich, UK, 1990.

[5] Maissan, J. F.: Wind Power Development in Sub-Arctic Conditions with Severe Rime Icing, TSYE Corporation - Circumpolar Climate Change Summit and Exposition, 2001.

[6] L. E. Kollar, R. Mishra: Inverse design of wind turbine blade sections for operation under icing conditions, Energy Conversion and Management (2019) DOI: 10.1016/j.enconman.2018.11.015

[7] A. Meana-Fernández, J. M. F. Oro, K. M. A. Díaz, S. Velarde-Suárez: Turbulence-Model Comparison for Aerodynamic-Performance Prediction of a Typical Vertical-Axis Wind-Turbine, Airfoil, Energies (ISSN 1996-1073) (2019) DOI:10.3390/en12030488

[8] S. Jain, N. Sitaram, S. Krishnaswamy: Effect of Reynolds Number on Aerodynamics of Airfoil with Gurney Flap, International Journal of Rotating Machinery, (2015) DOI: 10.1155/6149

[9] J. Nikuradse: Laws of Flow in Rough Pipes, NACA, Washington (1950)

[10] Introduction to ANSYS Fluent - Turbulence Modeling, ANSYS, Canonsburg, Pa, USA, (2014)

[11] ANSYS FLUENT Theory Guide, ANSYS, Canonsburg, Pa, USA, (2014)

[12] Spalart P. R. and Allmaras S. R., A one-equation turbulence model for aerodynamic flows, AIAA, vol. 092, no. 0439, (1992) DOI:10.2514/6.1992-439

[13] M. Drela, XFOIL: An Analysis and Design System for Low Reynolds Number Airfoils, Conference on Low Reynolds Number Aerodynamics, University of Notre Dame (1989) DOI:10.1007/978-3-642-84010-4_1

a. Airfoil Tools - NACA 4412 Xfoil prediction polar at RE=1,000,000,

[14] http://airfoiltools.com/polar/details?polar=xf-naca4412-il-1000000

[15] I. H. Abbott, A. E. von Doenhoff: Theory of Wing Sections - Including a Summary of Airfoil Data (1959)